

Non-Equilibrium Greens Function Approach to Majorana Bound States in 1D nanowires

Hamd Vakili^{*§}, Samiran Ganguly[†], Bhaskaran Muralidharan[‡], Avik W. Ghosh^{*†}

^{*}Dept. of Physics, University of Virginia, Charlottesville, VA, USA

[†]Charles L. Brown Dept. of Electrical and Computer Engineering, University of Virginia, Charlottesville, VA, USA

[‡]Dept. of Electrical Engineering, IIT Bombay, Powai, Mumbai-400076, India

[§]Email (corresponding author): hv8rf@virginia.edu

Abstract—Majorana bound states have been proposed as a candidate for topological quantum computing (QC), a QC paradigm where qubits are topologically protected against dephasing compared to non-topological QC. This can enable low error QC where the number of physical q-bits required is significantly smaller. N-S-N nanowires (Kitaev Chain) have been proposed as a device for topological QC. In this work, we build a Non-Equilibrium Greens Function (NEGF) based simulation platform that incorporates elastic dephasing using the self-consistent Born approximation (SCBA) and find Majorana modes to be robust against dephasing. We also compare the calculated conductance of the N-S-N system as a function of energy and applied magnetic field with predictions in the literature.

Index Terms—Majorana Zero Modes, NEGF, Kitaev Chain, Dephasing, Majorana Nanowire, Incoherent Quantum Transport

I. INTRODUCTION

Kitev chains are archetypical topological superconductors, and the analysis of N-S-N systems featuring Kiteav chains provides key insights into transport signatures of MZMs. These Majorana modes are topologically protected against local disorders and dephasing due to nonlocal entanglement, making them potentially robust candidates for q-bit systems for QC. Topological QC promises to reduce the number of physical q-bits required to build a feasible and useful QC system as compared to other candidate q-bit systems without such topological protection, such as trapped ions, coherent photons and Josephson junctions. It is expedient to build a quantum transport simulation platform that can incorporate realistic effects such as dephasing and braiding operations to explore system design choices. In this work, we present an important step toward developing a realistic simulation platform via the inclusion of phase and momentum relaxation effects. [1]–[4]

II. SCBA-NEGF SIMULATIONS FOR MAJORANA MODES

Kitaev Chain: We develop a NEGF formulation of the problem by setting up a two-band effective mass tight-binding Hamiltonian in the electron-hole Nambu space for the N-S-N structure. The N contacts to the S wire are assumed to be in equilibrium and are included phenomenologically using a given outflow rate. We then include non-dissipative dephasing

electron-electron/hole-hole interactions and elastic isotropic momentum scattering using the SCBA approach that accounts for all orders of Feynman diagrams of non-crossing terms, yielding a true bottom-up quantum mechanical simulation of the carrier transport in Kitaev chains. **Spin nanowire:** Equivalent system to the Kitaev chain which is widely used in experiments is a combination of a conventional s-wave superconductor (e.g. Nb), an axial magnetic field and spin orbit coupling to create a topological superconductor with protected mid-gap metallic Majorana modes. The 1D Hamiltonian can be written as $H = (-p_x^2/2m - \mu + \alpha p_x \sigma_y) \tau_z + B_x \sigma_x + \Delta \tau_x$, where σ and τ denote the Pauli matrices for spin and electron-hole space, respectively. p is momentum, α is the spin-orbit coupling. We discretize it in the x direction with the standard finite difference method (Figure 1). [5]–[10]

III. METHOD DESCRIPTION

We use a tight-binding model for the Hamiltonian (Figs. 3.d and 4.c). To calculate the transport signatures of the system the NEGF formalism is employed [9, 10]. The retarded Green function is defined as $G^R = [E - H - \Sigma_L - \Sigma_R - \Sigma_S]^{-1}$, where E is energy and $\Sigma_{L,R}$ are the contact self-energy terms and their anti-Hermitian parts $\Gamma = i(\Sigma - \Sigma^+)$ represent the escape rates into the leads and associated level broadening. We use a standard recursive surface Greens function to incorporate semi-infinite leads in $g_R = \beta g_R \beta^+$, $g_L = \beta^+ g_L \beta$, with the recursion equations $g_L = [E - H - \beta g_L \beta^+]^{-1}$, $g_R = [E - H - \beta^+ g_R \beta]^{-1}$, where α, β are onsite energy and hopping terms of the contacts, respectively. It is well known that Majorana zero modes are sensitive to impurities in the material. Here we propose three types of scattering that we incorporate into the NEGF formalism. The scattering term can in general be written as $[\Sigma_S]_{ij} = D_{ijkl} [G^R]_{kl}$ assuming the interacting sources are in equilibrium and elastic. Here $D_{ijkl} = \langle U_{ik} U_{jl} \rangle$ is the scattering term, a bilinear thermal average over the scattering potential U_{ij} between sites i and j . The form of D determines the scattering behavior. For spatially localized scattering, $U_{ij} = U_i \delta_{ij}$, and $D_{ijkl} = D_{ij} \delta_{ik} \delta_{jl}$ turns into a second rank matrix D_{ij} rather than a fourth rank tensor. Note that the Σ_S needs to be calculated self-consistently, as it depends on GR which in turn depends on Σ_S . Ignoring self-consistency will cause current leakage into the virtual

scattering contact that should only act as a randomizing voltage probe. The local density of state (LDOS) is calculated from diagonal elements of $A(E) = i[G^R - G^A]/2\pi$ where $G^A = G^{R\dagger}$. Finally, the electron transmissions are calculated using the Fisher-Lee formula for the coherent transport, $T_{ab}(E) = \text{Trace}(\Gamma_{ia}G^R\Gamma_{jb}G^A)$ and conductance as $G_{ab} = \frac{e^2}{\hbar}T_{ab}$, where electrons crossing contacts ($i=1, j=2, a=b=e$ or h) represent direct transmission, transforming into holes at the same contact (e.g. $i=j=1, a=e, b=h$) represent Andreev Reflection, and transforming across contacts represent Crossed Andreev transmission ($i=1, j=2, a=e, b=h$). [11]–[13] For the non-coherent cases we use the equation:

$$I_L = \frac{1}{2} \left[\frac{e}{\hbar} \text{Tr}(T_z [G^R \Sigma_L^< - \Sigma_L^< G^A + G^< \Sigma_L^+ - \Sigma_L G^<]) \right] \quad (1)$$

with

$$T_z = I \otimes \tau_z, \quad \Sigma_{L,R}^<(E) = i\Gamma_{L,R} f_{L,R}(E) \quad (2)$$

$$G^<(E) = G^R(E)(\Sigma_L^<(E) + \Sigma_R^<(E))G^A(E) \quad (3)$$

The total conductance is then calculated from the general formula $G(V) = \frac{\partial I}{\partial V}$.

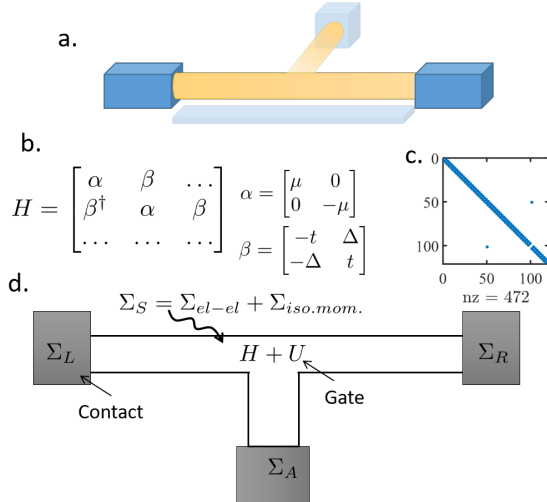


Fig. 1. (a) N-S-N structure or Kitaev chain under study. Enhancements include a second orthogonal arm and gate potential. (b) The Hamiltonian of the 1D nanowire: SOC + s-wave + magnetic field (c) Hamiltonian in the effective mass tight-binding Nambu space representation (spins not shown), with superconducting gap occurring in the off-diagonal terms. (d) Visual representation of the Hamiltonian in a sparse matrix representation. The two arms of the system (main arm and side arm) are connected using a far off-diagonal term. (e) NEGF setup for the system. The normal-metal contacts are represented using self-energies, dephasing and momentum scattering included using a self-energy using SCBA.

IV. RESULTS

Here we represent a demo of our results based on the methods described above. Showing the predicted transport signatures of MZM such as the quantized conductance (Figure 2), localized LDOS (Figure 3) and the topological transition by changing the magnetic field (Figure 4). Figure 2 and 3 are for Kitaevs chain as described by Fig 1.c. Figures 4-7

are for 1D Majorana nanowire, Fig1.b. To further expand the method described earlier we apply pure phase and momentum scattering terms to the Majorana nanowire system. [14]

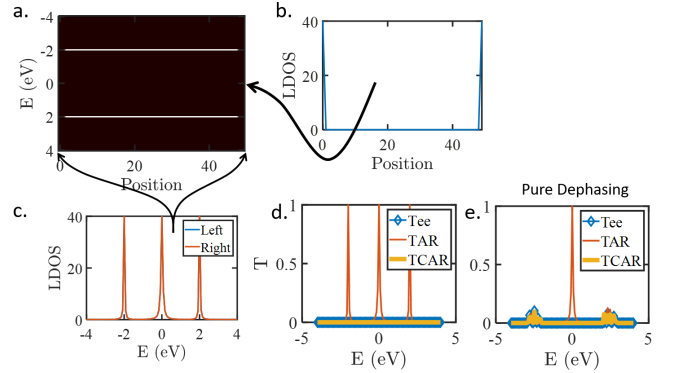


Fig. 2. Local density of states (LDOS) plot for the nanowire resolved energetically and positionally for a coherent simulation. Electron and hole bands can be clearly seen. (b) LDOS plot at 0 energy axis shows Majorana zero energy modes (MZM). (c) MZM along with electron and hole levels seen at left and right edges of the nanowire. (d) Electron-electron, Andreev and Cross Andreev Reflections (Tee, TAR, TCAR respectively), showing signature of MZM.

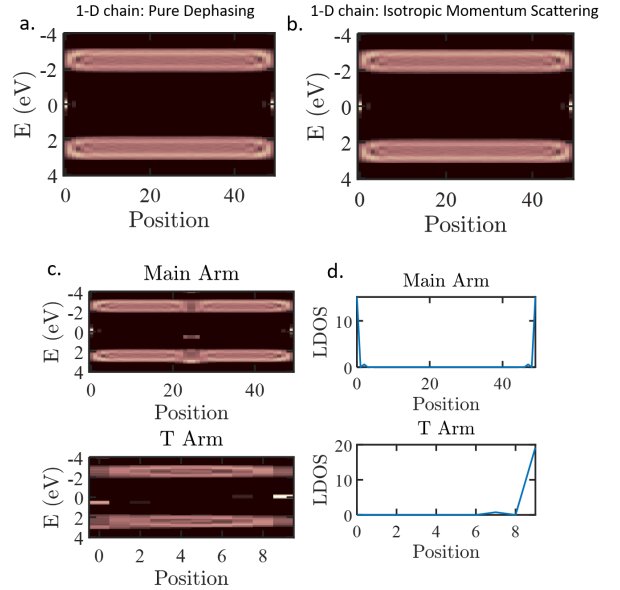


Fig. 3. (a) and (b) LDOS of the nanowire under pure dephasing (i.e. no loss of momentum) and isotropic momentum scattering, with broadened levels. MZM can be clearly discerned localized at 0 energy and at the edges. (c) LDOS for the Main and T arms in a T junction structure under pure dephasing. MZMs at the edges of the main arm and at the end of the T arm can be clearly discerned. There is a non-zero mode coupling state at junction point which is not a Majorana mode. (d) LDOS plots in main and T arms at 0 energy axis.

A. MNW Phase + momentum scattering

By using $D_{ij} = D_p \delta_{ij}$ (zero for electron-electron or hole-hole cross-terms) we can add the momentum relaxation terms to the Majorana nanowire Hamiltonian (Fig 1.b) as described, here we show the results for the total transmission

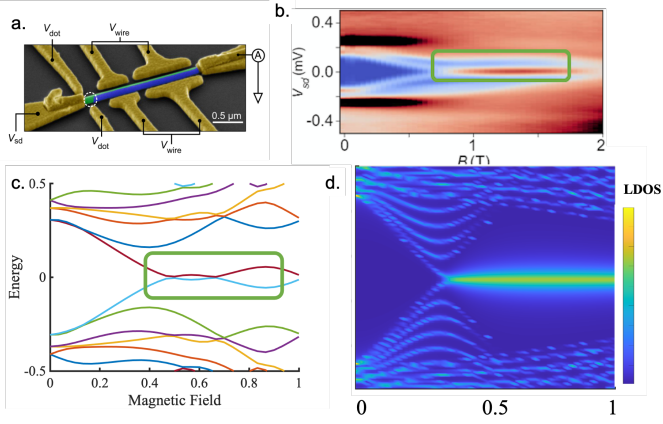


Fig. 4. (a) The experimental setup of a 1D Majorana nanowire. (b) Shows the energy spectrum vs magnetic field. Note that the crossing itself is not indicative of existence of Majorana zero mode. The oscillatory behavior as seen in (c) is required which needs a higher quality material. (c) The energy spectrum from numerical calculation assuming perfect conditions. (d) LDOS calculations, show a similar signature to experimental.¹²

and comparison with the case with no relaxation term. As seen from figure 5.a, a larger contact energy Γ results in broadening of the transmission vs magnetic field. By introducing a momentum relaxation term, the transmission falls below 1. The momentum relaxation term decreases the quantized signature of transmission and broadens the transmission vs magnetic field. In figure 6 we see the conductance color plots vs Energy and magnetic field, the lighter lines show the peaks in conductance. With no relaxation terms, Fig 6.a, we see that these lines are very thin. By adding a momentum relaxation term, Fig 6.b, the lines become thicker which is due to the broadening effect of relaxation terms. However the location of peaks and energy gap closings is unchanged from Fig 6.a to 6.b.

B. MNW Dephasing scattering

For pure dephasing terms, we use $D_{ij} = D_d$. As seen in figure 7.a, pure dephasing relaxation has a similar qualitative effect to momentum relaxation. But quantitatively we see that the pure dephasing has a more pronounced effect on the broadening of the conductance signature of MNW zero modes. In figure 7.b we can see that with relaxation terms, no matter the magnitude or type, the zero-mode LDOS localization is unchanged.

V. DISCUSSION AND CONCLUSION

In this work, we have considered non-coherent transport across topological superconductor based N-S-N systems. In the treatment of dephasing we considered two extremes: a) localized fluctuating scatterers giving rise to phase + momentum dephasing and b) strong non-local scatterers giving rise to phase relaxation. The computational technique developed here will lead to important tools to analyze Majorana based electronic devices in the realistic limit. A few interesting points regarding the physics must be taken note of. Firstly,

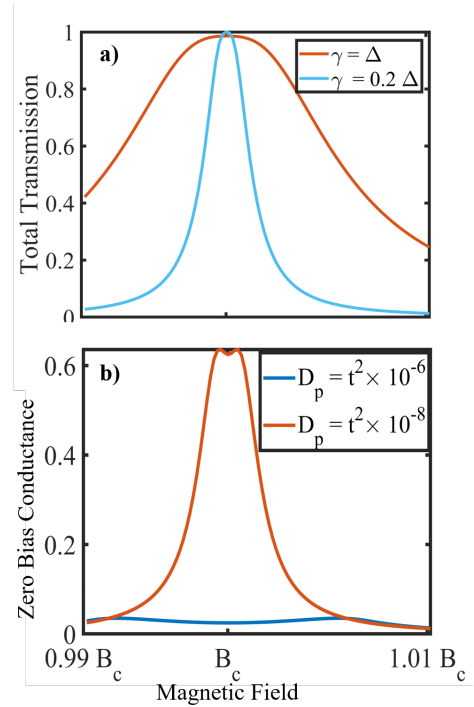


Fig. 5. Transmission signature around the critical magnetic field. a- shows the total transmission vs magnetic field for two different values of gamma which corresponds to the broadening of the transmission. b- shows the effect of momentum relaxation, which shows that for a too-large momentum relaxation the quantized transmission no longer exists. B_c is the critical magnetic field where the gap closing happens as seen in figure 4.d.

the scattering processes are taken with respect to electronic fluctuating Coulomb forces, which are not related to the pairing processes leading to superconductivity. In such cases, the scattering terms do not include those involving the pairing processes, such that the entire self energy matrix is block diagonal within the electron and hole blocks of the BdG representation. Furthermore, advancements in quantum transport simulations are needed to include a self consistent treatment of the order parameter, along with realistic multi-modal effects in the nanowires. Ultimately a fully self consistent treatment of the Poisson equation and the pairing interaction will be an important advancement for modeling of a realistic Majorana nanowire device, much needed to support today's experimental efforts. We have shown the NEGF tool can be expanded to be used for Kitaev chains and MNW with various relaxation terms by using self-consistent Born approximation (SCBA). We have studied the effects of two types of relaxation here, but in principle, it can be extended to include any relaxation term describable by perturbation theory. Both momentum and pure dephasing relaxation terms studied here have qualitatively similar effects on broadening the conductance of MNW and lowering the peaks. However, the MZMs still exist even with relaxation terms which is indicative of their topological nature. The NEGF method can be used to study transmission signatures of more complicated structures such as T-junctions or 2D materials. The NEGF method can also be expanded,

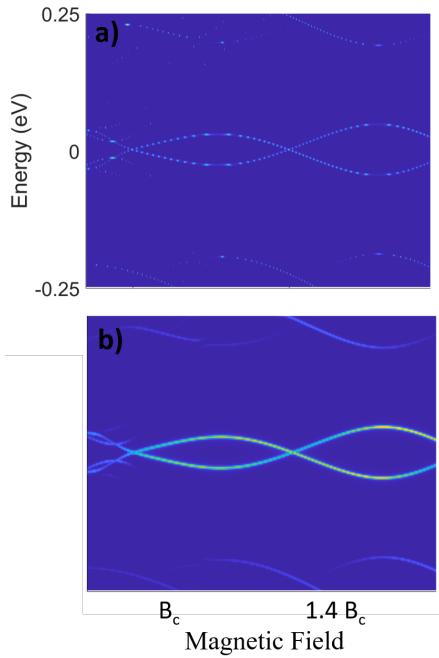


Fig. 6. A color plot of total conductance for Energy vs magnetic field. a) Without relaxation terms the lines are very thin which is indicative of the quantized conductance behavior. In contrast with momentum relaxation ($10^{-6} t^2$), the lines are broadened (thicker lines). The existence of the energy gap closing at critical magnetic fields shows that the Majorana zero mode still exists in the nanowire albeit with a weaker signature. At the parity crossings the conductance peaks still exist (not visible in the figures)

based on the same theoretical frameworks, to include time-evolving effects (TDNEGF), to study the non-abelian statistics of braidings.

ACKNOWLEDGEMENTS

This work is funded in part by the Defense Advanced Research Projects Agency (DARPA) Topological Excitations in Electronics (TEE) program (grant D18AP00009).

REFERENCES

- [1] J. Alicea, "New directions in the pursuit of majorana fermions in solid state systems," *Reports on Progress in Physics*, vol. 75, no. 7, p. 076501, Jun 2012. [Online]. Available: <https://doi.org/10.1088/0034-4885/75/7/076501>
- [2] M.-T. Deng, S. Vaitiekėnas, E. Prada, P. San-Jose, J. Nygård, P. Krogstrup, R. Aguado, and C. M. Marcus, "Nonlocality of majorana modes in hybrid nanowires," *Phys. Rev. B*, vol. 98, p. 085125, Aug 2018. [Online]. Available: <https://link.aps.org/doi/10.1103/PhysRevB.98.085125>
- [3] T. C. Bartolo, J. S. Smith, B. Muralidharan, C. Müller, T. M. Stace, and J. H. Cole, "Aharonov-Bohm interference as a probe of majorana fermions," *Phys. Rev. Research*, vol. 2, p. 043430, Dec 2020. [Online]. Available: <https://link.aps.org/doi/10.1103/PhysRevResearch.2.043430>
- [4] N. Leumer, M. Grifoni, B. Muralidharan, and M. Marganska, "Linear and nonlinear transport across a finite Kitaev chain: An exact analytical study," *Phys. Rev. B*, vol. 103, p. 165432, Apr 2021. [Online]. Available: <https://link.aps.org/doi/10.1103/PhysRevB.103.165432>
- [5] T. D. Stanescu and S. Tewari, "Majorana fermions in semiconductor nanowires: fundamentals, modeling, and experiment," *Journal of Physics: Condensed Matter*, vol. 25, no. 23, p. 233201, May 2013. [Online]. Available: <https://doi.org/10.1088/0953-8984/25/23/233201>

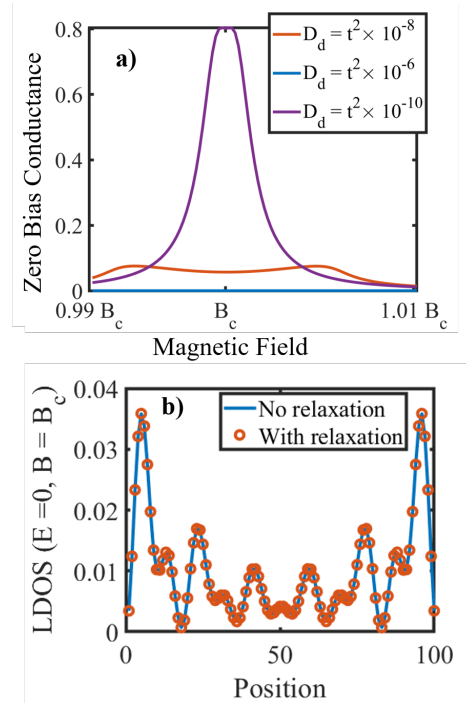


Fig. 7. a) Introducing pure dephasing relaxation terms have a qualitatively similar effect to momentum relaxation. However, the dephasing term has a stronger broadening effect. b) With all of the relaxation terms discussed in this paper, the Majorana zero mode LDOS is unchanged which shows their topological nature.

- [6] S. D. Sarma, M. Freedman, and C. Nayak, "Majorana zero modes and topological quantum computation," *npj Quantum Information*, vol. 1, no. 1, p. 15001, Dec. 2015. [Online]. Available: <http://www.nature.com/articles/npjqi20151>
- [7] . Gl, H. Zhang, J. D. S. Bommer, M. W. A. de Moor, D. Car, S. R. Plissard, E. P. A. M. Bakkers, A. Geresdi, K. Watanabe, T. Taniguchi, and L. P. Kouwenhoven, "Ballistic Majorana nanowire devices," *Nature Nanotechnology*, vol. 13, no. 3, pp. 192–197, Mar. 2018. [Online]. Available: <http://www.nature.com/articles/s41565-017-0032-8>
- [8] M. Barkeshli, C.-M. Jian, and X.-L. Qi, "Twist defects and projective non-abelian braiding statistics," *Phys. Rev. B*, vol. 87, p. 045130, Jan 2013. [Online]. Available: <https://link.aps.org/doi/10.1103/PhysRevB.87.045130>
- [9] M. T. Deng, S. Vaitiekėnas, E. B. Hansen, J. Danon, M. Leijnse, K. Flensberg, J. Nygård, P. Krogstrup, and C. M. Marcus, "Majorana bound state in a coupled quantum-dot hybrid-nanowire system," *Science*, vol. 354, no. 6319, pp. 1557–1562, 2016. [Online]. Available: <https://science.sciencemag.org/content/354/6319/1557>
- [10] P. Sriram, P. S. Kalantre, K. Gharavi, J. Baugh, and B. Muralidharan, "Supercurrent interference in semiconductor nanowire Josephson junctions," *Phys. Rev. B*, vol. 100, p. 155431, Oct 2019.
- [11] S. Datta, *Lessons from Nanoelectronics*. WORLD SCIENTIFIC, 2012. [Online]. Available: <https://www.worldscientific.com/doi/abs/10.1142/8029>
- [12] A. Ghosh, *Nanoelectronics*. World Scientific, 2016. [Online]. Available: <https://www.worldscientific.com/doi/abs/10.1142/10152>
- [13] C. Duse, P. Sriram, K. Gharavi, J. Baugh, and B. Muralidharan, "Role of dephasing on the conductance signatures of Majorana zero modes," *Journal of Physics: Condensed Matter*, vol. 33, no. 36, p. 365301, Sept. 2021. [Online]. Available: <https://iopscience.iop.org/article/10.1088/1361-648X/ac0d16>
- [14] H. Zhang, D. E. Liu, M. Wimmer, and L. P. Kouwenhoven, "Next steps of quantum transport in Majorana nanowire devices," *Nature Communications*, vol. 10, no. 1, p. 5128, Dec. 2019. [Online]. Available: <http://www.nature.com/articles/s41467-019-13133-1>